Characterization of GPS multipath for passenger vehicles across urban environments

Olivier Le Marchand, Philippe Bonnifait, Javier Ibañez-Guzmán, David Betaille, François Peyret

Characterization of GPS multipath for passenger vehicles across urban environments

Olivier Le Marchand[1], Philippe Bonnifait[2], Javier Ibañez-Guzmán[1], David Bétaille[3], François Peyret[3]
[1]*Renault S.A.S., Guyancourt, France*
[2]*Heudiasyc UMR 6599, Université de Technologie de Compiègne (UTC), France*
[3]*Laboratoire Central des Ponts et Chaussées (LCPC), Nantes, France*

***Abstract*— Multipath signals have a strong effect on position estimates; these are studied intensely theoretically and experimentally. In this paper a domain oriented perspective is presented, passenger vehicles traversing dense urban areas. The purpose is to examine the effects of multipath on pseudo-ranges and Doppler measurements. The approach combines a theoretical formulation with extensive testing. The experiment includes the acquisition of measurements provided by a low-cost automotive GPS receiver on-board a vehicle in real traffic conditions. In addition, the vehicle trajectory was measured precisely to allow for the quantification of measurement errors. Two approaches are used in the experimental part to determine the pseudo-range and Doppler errors: Vehicle on-board measurements plus post-processing; vehicle on-board measurements, data from an external GPS reference station and post-processing. The results enable the identification of satellites whose signals are corrupted by multipath, to plot the results with respect to the trajectory so as to provide contextual information that facilitates understanding. It was also possible to establish the discontinuous relationship between signal to noise ratio and pseudo-range & Doppler errors.**

I. INTRODUCTION

For a passenger vehicle, the main source of absolute position information is provided by GNSS signals. When signal occlusion or multipath occurs, these will lead to position estimation errors. When deploying safety-related and location dependent vehicle navigation applications, ensuring the information integrity and hence detecting errors is a major requirement [1], [2]. Further, a thorough performance evaluation of GNSS receivers operating in normal traffic conditions has shown that standard deviations recorded from the receivers do not reflect the true error of the vehicle trajectory [3]. Thus, the characterization of these errors remains a major challenge.

The civil aviation domain has introduced the concept of integrity since the early 90s to estimate the level of trust on the location estimations. To increase integrity, a conventional approach relies on the use Fault Detection and Exclusion (FDE) algorithms. This is suitable for detecting and rejecting errors caused by the immediate environment around the receiver. The approach has shown the potential risks associated to situations where biases are undetected. In an automotive context biases often occur due to multipath when traversing densely built areas, thus it is very important to be able to remove them. For this purpose, the effects of multipath on the pseudo-ranges and Doppler need to be understood. It will be then possible to develop efficient FDE mechanism that correspond to the automotive domain.

The multipath effects on GNSS receivers has been studied at different levels from a signal analysis perspective and mainly applied to fixed position test condition. These studies have included issues related to the Radio Frequency (RF) part of the receivers, the effects of multipath on pseudo-range information and Carrier Phase measurements [4] [5]. Multiple simulations have also been developed to address the subject [6] [7]. In this paper, these studies are extended to the use of GNSS receivers when applied to passenger vehicles. That is GPS receivers are mounted on a passenger vehicle moving at speed in standard traffic conditions inside an urban area. The analysis can be considered as vehicle specific. It takes into account kinematic constraints as well as the use of low-cost automotive type receivers.

In this paper, two new methods are proposed to characterize the multipath received by a GPS on-board a mobile platform traversing a densely built area. They address the effects of multipath on the pseudo-range and the Doppler measurements. Both are relying on a set of assumptions and on the recording of a precisely measured vehicle trajectory as the ground truth with respect to which errors are measured and analyzed. In addition, the second method relies on data col-

lected by a GPS fixed reference station located within the proximity of the test area. A description of the equipment used for recording and post-processing of the data is includes, as it is an important component of our approach. Tests have been performed in a typical urban environment to validate both methods. The spatial-urban characteristics of the test environment is also described in detail. The results are used to compare the relevance of both methods. To provide a better understanding of the relationships between the multipath and the surrounding environment a 3D analysis was established. This was made by relating the vehicle pose with the corresponding measurement errors. The relationship bee tween the Signal to Noise Ratio (SNR) and error magnitudes due to multipath are also examined.

The remainder of the paper is organized as follows: Section II describes both methods as well as the related assumptions. Section III introduces the experimental setup used for this evaluation. The details of the trajectory to which the methods are applied is described in detail in Section IV, including information on the satellite configuration available during the data logging period. The results obtained are presented and analyzed in Section V. Finally, a critique on the methods is made as well as conclusions on the findings with regard to the GPS operation from the usage of such information for passenger vehicle applications.

II. Multipath estimation methods

Multipath is considered as the first disturbance issue at the receiver level, and has been in interest since several decades [8]. While this issue received much interest in static conditions of observation (particularly with tests that already demonstrated their impact on the pseudo-ranges), in this article, we will focus on a moving vehicle and we will consider a dynamic context. Hence, estimation techniques of multipath characteristics have to be adapted. The theoretical pseudo-range model considered in our investigations is first presented. Then two different methods that estimate the consequences of multipath on code measurements are explained. And finally we demonstrate how they can be adapted to encompass also the consequences of multipath on Doppler measurements.

A. Pseudo-range model

Several pseudo-range models have been proposed in the literature. Their differences reside in the complexity of the representation of the physical phenomena that intervene during the signal in space propagation [9]. The model must reflect the precision of the instrumentation used in the experimental phase as well as the expected accuracy of the tested GPS receiver, a low cost automotive receiver. Within these considerations, all the delays and constraints linked to the receiver RF components are neglected together with delays due to the center of phase of antennas. The pseudo-range model used is limited to:

$$\rho_i^u = d_i^u + c.dt_i + c.dt^u + \Delta atmo_i^u + \Delta m_i^u + \epsilon_i^u \quad (1)$$

where u is the receiver index (this can be either v for the vehicle or b for a local base station), i the satellite index, ρ the pseudo-range measurement, d the true distance between the receiver and the satellite, c the speed of the light, dt the clock offset (either of the satellite or of the receiver), $\Delta atmo$ the ionospheric and tropospheric added delays in meters, Δm the multipath delay in meters, and ϵ_i^u representing the receiver noise.

B. Receiver autonomous method

To remove the unwanted biases from the model proposed in Equation 1, the following assumptions are taken for this method:

1) The GPS antenna position can be measured with an accuracy of an order of magnitude of half a meter during the whole trajectory. Therefore d_i^u can be considered as known.
2) The correction of the satellite clock offset by the broadcasted GPS data is considered to be sufficient, i.e. $c.dt_i$ is removed.
3) The standard modeling of the atmospheric biases is considered to be sufficient, so $\Delta atmo_i^u$ is corrected.
4) At least one satellite signal is assumed to be free of multipath at each epoch of the trajectory, this can be expressed as $\exists i$ such as $\Delta m_i^u = 0$

The estimation of the pseudo-range model is regarded as a four steps method:

First Step. It consists on making a coarse estimation of the receiver clock offset. The usual position problem of the GPS is solved applying a least squares algorithm based on the linearization of the observation function:

$$\begin{bmatrix} \rho_1 \\ \vdots \\ \rho_N \end{bmatrix} = H \begin{bmatrix} x \\ y \\ z \\ c.dt^v \end{bmatrix} \quad (2)$$

Because of the first hypothesis, x y and z are known, so the distance d between the satellite and the receiver can be computed for each satellite. Taking in account the second and the third assumptions, a first estimate of the receiver clock offset $\hat{dt^v}$ is obtained by simply averaging the residual distance:

$$c.\hat{dt^v} = \frac{1}{N}\sum_{i=1}^{N}(\rho_i^v - d_i^v) \tag{3}$$

which leads to the following equation with the help of the second assumption:

$$c.\hat{dt^v} = \frac{1}{N}\sum_{i=1}^{N}(c.dt^v + \Delta m_i^v + \epsilon_i^v) \tag{4}$$

where N is the number of satellites.

In the second step, one has to empirically separate the subset of satellites that are not subject to multipath during a certain time period in the track. Applying the previous estimation of the receiver clock offset, a first coarse estimation of the multipath magnitude $\Delta\hat{m}_i^v$ on each satellite can be made:

$$\Delta\hat{m}_i^v = \rho_i^v - d_i^v - c.\hat{dt^v} \tag{5}$$

$$\Delta\hat{m}_i^v = \Delta m_i^v + \epsilon_i^v - \frac{1}{N}\sum_{j=1}^{N}\left(\Delta m_j^v + \epsilon_j^v\right) \tag{6}$$

This estimation is clearly insufficient to provide a detailed analysis of multipath. Nevertheless, the visual comparison of $\Delta\hat{m}_i^v$ time series permits an approximate identification of multipath-free satellites.

The third step provides a precise estimate of the receiver clock offset. Equation 3 is applied with the only N^m satellites identified as multipath free. In order to verify that the identification is correct, the second step can be repeated with the new $c.\hat{dt^v}$ estimation. Thus, multiple iterations of the first and second steps can be necessary in order to converge. For difficult cases, it can be necessary to change the subset of satellites along the trajectory to obtain a relevant estimation of $c.\hat{dt^v}$.

Fourth Step: Finally the multipath magnitude is computed with the reliable receiver clock estimation and is equal to:

$$\Delta\hat{m}_i^v = \Delta m_i^v + \epsilon_i^v - \frac{1}{N^m}\sum_{k=1}^{N^m}(\epsilon_k^v) \tag{7}$$

The ability to estimate multipath magnitude has to be balanced with respect to the root hypothesis. The more fault free satellites we have, the more accurately the receiver clock offset will be estimated. In a similar manner, it can be stated that, the more hypothesis are respected, the more precise the $c.\hat{dt^v}$ estimation will be. In such cases the estimate of the multipath magnitude will also be optimized. The hypotheses aforementioned are also of key importance in the success of the method, as it will be demonstrated in Section V.

C. Double difference based method

Another way of performing multipath magnitude estimation is to make use of an additional base GPS receiver. The principle is to perform double differences [9], as it allows for the efficient removal of disturbances and to obtain more accurate and precise estimations. The application scheme of this method is similar to the earlier one as it is also based on a set of hypothesis which are as follows:

1) The position of the vehicle receiver antenna is known with an accuracy of half a meter during the whole trajectory, thus $d_i^v$is known.
2) The position of the base receiver antenna is known, so similarly d_i^b is known.
3) All the satellite signals received at the base station are supposed to be multipath free, i.e. $\forall i, \Delta m_i^b = 0$
4) The distance between the vehicle and the base is sufficiently small to assume that they are affected by the same atmospheric biases, i.e. $\forall i, \Delta atmo_i^b = \Delta atmo_i^v$.
5) At least one of the satellite signals received at the vehicle is assumed to be free of multipath at each epoch of the trajectory, i.e. $\exists i$ such as $\Delta m_i^v = 0$.

The fault free satellite mentioned in the fifth assumption will be used as the reference one for computing the double difference at this epoch: it will be noted with subscript p. The double difference of pseudo-ranges $\triangle\nabla\rho_{i,p}^{u,w}$ of any satellite regarding to the reference one, applied to two receivers u and w is defined as:

$$\rho_{i,p}^{u,w} \hat{=} \triangle\nabla\rho_{i,p}^{u,w} = \rho_i^u - \rho_i^w - \rho_p^u + \rho_p^w \tag{8}$$

The simplified algebraic representation of the double difference $\triangle\nabla$ is further applied to other variables. With respect to equation 1, and after removing the common clock terms, the double difference can be expressed as:

$$\begin{aligned}\rho_{i,p}^{v,b} = \quad & d_i^v - d_i^b - d_p^v + d_p^b \\ & + \Delta atmo_i^v - \Delta atmo_i^b - \Delta atmo_p^v + \Delta atmo_p^b \\ & + \Delta m_i^v - \Delta m_i^b - \Delta m_p^v + \Delta m_p^b \\ & + \epsilon_i^v - \epsilon_i^b - \epsilon_p^v + \epsilon_p^b \end{aligned} \tag{9}$$

If the previous assumptions are taken in account together with the absence of multipath on p satellite at the vehicle, it can be simplified, leading to :

$$\rho_{i,p}^{v,b} = d_{i,p}^{v,b} + \Delta m_i^v + \epsilon_{i,p}^{v,b} \tag{10}$$

from where an estimate of the magnitude of multipath on satellite i can be extracted straightforwardly, as $\rho_{i,p}^{v,b}$ and $d_{i,p}^{v,b}$ are known:

$$\Delta \hat{m}_i^v = \rho_{i,p}^{v,b} - d_{i,p}^{v,b} \tag{11}$$

The first step of the method is to find in an trial-and-error manner a fault free satellite, as in the previous method. It consists in visually identifying the absence of jump in a time series of $\rho_{i,k}^{v,b} - d_{i,k}^{v,b}$. This would lead to the conclusion that both i and k satellites are multipath free. The comparison of one particular satellite to many other is sometime necessary to demonstrate the absence of multipath on it during the whole trajectory. Moreover it can be necessary to change the reference satellite during the tracking period. In practice, the highest satellites will have the highest probability to be fault free, thus to be preferably used as the reference satellite.

The second step is the computation of the multipath estimation with respect to the previously identified reference satellite and the Equation 11.

D. Error on Doppler measurements

In a similar manner as Equation 1, the Doppler measurements are linked to the unknowns by:

$$\begin{aligned} Dop_i^u = (\vec{v_i} + \vec{v}^u) \,.\vec{u}_i^u + c.ddt_i + c.ddt^u + ... \\ \Lambda atmo_i^u + \Lambda m_i^u + \epsilon_i^u \end{aligned} \tag{12}$$

where Dop is the Doppler measurement, $\vec{v_i}$ the velocity vector of the satellite, $\vec{v}^u$ the velocity vector of the receiver, $\vec{u}_i^u$ the unitary support vector from the receiver to the satellite, ddt the satellite clock drift (either of the satellite or of the receiver), $\Lambda atmo$ the ionospheric and tropospheric effects on the Doppler in meters per seconds, Λm the impact of the multipath in meters per seconds, and ϵ_i^u which is the receiver noise on Doppler. Consequently, the same reasoning from both previous methods can be applied to the Doppler measurements. Biases can be corrected from broadcasted data or neglected (such as $\Lambda atmo_i^u$), then the receiver clock drift is estimated with the help of the knowledge of the vehicle motion, what leads to an estimation of Λm_i^v. This represents the first method. For the second one, double differences can be straightforwardly applied, leading to:

$$\Lambda \hat{m}_i^v = \frac{c}{L}.Dop_{i,p}^{v,b} - \nabla\triangle \left[(\vec{v_j} + \vec{v}^u) \,.\vec{u}_j^v \right]_{i,p}^{v,b} \tag{13}$$

where L is the frequency of the carrier phase from which the Doppler is measured.

III. Experimental setup

The experimental setup was designed to be automotive applications oriented. This consideration implies that a passenger vehicle was to be driven through typical traffic conditions and was to be equipped with automotive type GPS receivers. The vehicle position was measured by high accuracy equipments and the estimations are enhanced to reach centimeter level accuracy applying post-processing techniques. This so computed trajectory is referred as the ground truth. The estimates from the GPS receiver to be analyzed are compared with regard to this ground truth. In the next sections the measuring systems used are described in detail followed by the post-processing process.

A. Measuring systems

Two types of measurements are made as part of the experiment. The first one measures the vehicle location as it traverses the test areas as well as outputs of the on-board GPS receivers. The second one consists of a base station GPS receiver for reference purposes.

The reference trajectory can be estimated in real-time by an inertial based positioning system, known as LandINS. This consist of a loosely coupling between a strap-down Inertial Measurement Unit (IMU), a GPS and a vehicle odometer. The system can generate pose estimations in real-time with a precision less than 1 m. The IMU consists of three pendulum accelerometers and three navigation-grade fiber-optic gyroscopes, it is manufactured by IXSEA [10]. The accuracy of these position estimates can be enhanced up to a centimeter level accuracy using post-processing techniques, what is required for our study. For this purpose, it is necessary to record the dynamic response of the vehicle using the IMU with data recorded at 100 Hz together with GPS data and the vehicle odometer. The later uses a dual-frequency receiver (a Novatel OEM4) that

provides raw data of code and phase. The reference frame attached to the IMU is shown in Figure 1.

In order to obtain a such accuracy and precision, all the data used in the computation has to reach the same level of accuracy and precision. Consequently, GPS reference data is collected during the period of the test trials nearby a GPS reference station of the French "Réseau GPS Permanent" (RGP). It allows computing a first PP Kinematic GPS trajectory. In addition, the spatial descriptions between the LandINS GPS antenna and the automotive GPS antennas were measured with high precision (centimeter level) with respect to the IMU reference frame. Finally, the odometer was calibrated by driving the vehicle at a constant speed on a 1km long straight line.

Every data is timestamped so it can be associated and fused as part of the post-processing process.

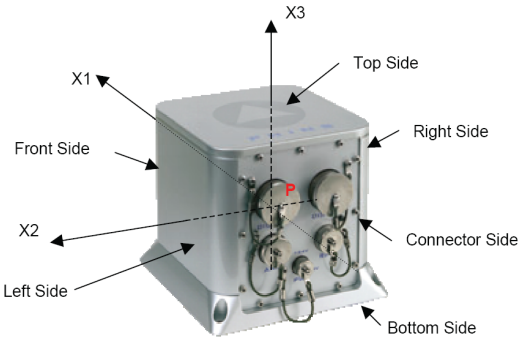

Fig. 1. LandINS reference frame

B. Post-processing

The post-processing allows the reconstruction of the vehicle trajectory using the measurements stored during the trials. After collecting raw IMU data, raw GPS data from the on-board GPS receiver, and raw GPS data from a base station, the whole data set is tightly coupled with the help of "Inertial Explorer" software. Inertial Explorer post-processing software suite is developed by Waypoint Products Group's [11]. It integrates data from six degrees of freedom IMU with GNSS information processed with an integrated GNSS post-processor similar to GrafNav product. It implements tightly coupled (TC) processing that uses GPS carrier phase and solves the ambiguity resolution problem on the fly with an algorithm named Advance Real Time Kinematic (ARTK). This guarantees that the position error in presence of multipath (or when the satellite view is occluded) will be limited to 20 centimeters regarding to our experimental conditions, and significantly reduced compared to real-time solutions.

C. Automotive type GPS

A thorough performance evaluation of automotive GPS receivers was made by the authors in [3]. Out of this characterization, the Ublox AEK-4T unit was selected. It provides access to pseudo-ranges and other embedded data. Two Automotive GPS receivers were mounted on the vehicle. They are connected to a single GPS antenna via an antenna splitter to have access to the same RF signal. One of the receiver was set up to operate at 1 Hz whilst the other at 10 Hz. For both receivers, the raw data, that is the pseudo-range, carrier phase, Doppler and SNR were recorded.

IV. Test Site

In dense urban environments due to the presence of high buildings there is a strong likelihood for the presence of multipath and the occlusion of GPS signals. The test site was chosen to reflect such a situation as in the case of the city of Saint Quentin en Yvelines (48°47'01.88" N, 2°02'35.32" E), France. The trajectory measured during the experiments is plotted in Figure 2. The vehicle crosses a large dense urban area, the trajectory is surrounded by tall modern office buildings. Several of these are lined with large glass windows which reflect the GPS signals and will be the cause of multipath. Of particular interest is a segment of this trajectory as it presents severe difficulties. As the vehicle enters the oval like area (labeled as the 'Plaza') , this is surrounded by buildings that occlude most satellite signals whilst at the same time reflecting several others. A satellite picture of this place is shown in Figure 3. A picture taken from the test vehicle is shown in Figure 4 to illustrate the characteristics of the surrounding buildings. The vehicle traveled for a period of 500 seconds at speeds between 30 to 50 Km/h.

Figure 5 provides an insight of the elevation and the azimuth of the GPS satellites during the trial. Two satellites (prn 20 and prn 11) have a high elevation and will be good candidates to be reference satellites, or to be used for the receiver clock parameters estimations.

V. Results

The results obtained from the analysis of the vehicle position estimates applying both methods on the automotive receivers are presented in this section. The different steps used in both methods are presented. The results are then compared and the differences analyzed. The characteristics of the errors observed are defined,

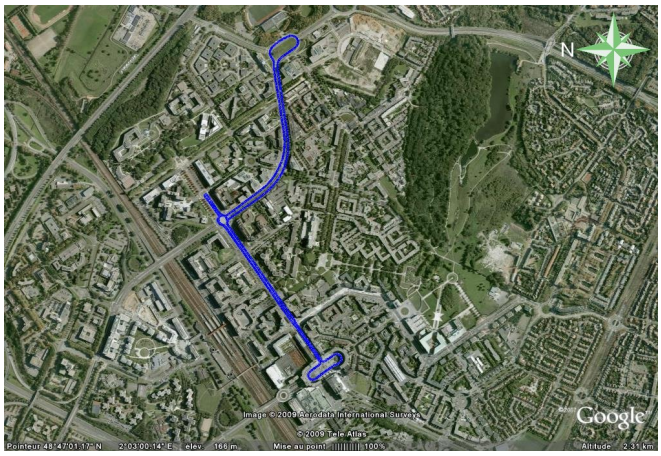

Fig. 2. Satellite view of the test track

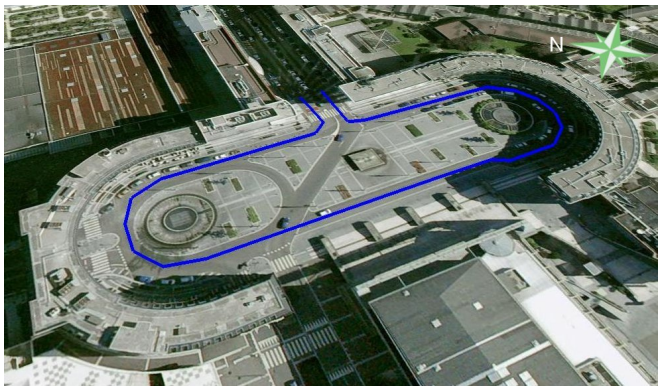

Fig. 3. Satellite view of the oval place with the reference trajectory

Fig. 4. Vehicle perspective picture within the oval place

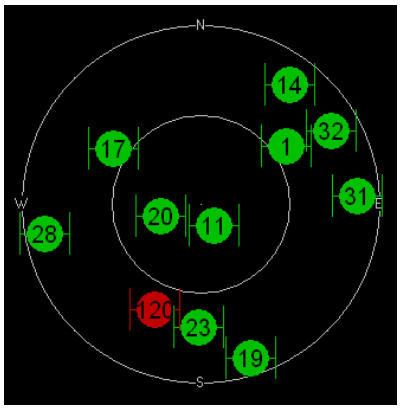

Fig. 5. Satellite view during the record

and analyzed with respect to the reference 3D vehicle position and its surrounding environment. Finally the link between these errors and Signal to Noise Ratio (SNR) is also made.

A. Application of the approach to the acquired data.

For the receiver autonomous method, the second steps consists in the coarse estimation of the delays in the pseudo-range signals. These, expressed in metres, are shown in Figure 6 for some representative satellites of the constellation (satellites prn 20, 17, 31 and 19). The automotive GPS receiver was set to operate at 1 Hz. It is to note that the plotted errors are computed as the ground truth value minus the measured one, so $error = -\hat{\Delta m}_i^v$: the reason for the NLOS multipath (which causes the measured value to be higher than the true one) to induce errors with negative values. If tracking of the observed satellite has been lost at the GPS receiver, by design the error value is set to 0. This is the reason for the sudden jumps to 0 in the plots. By visual inspection of the different satellites satellites in Figure 6, it can be inferred that multipath are affecting satellites prn 31 and 19, whilst still no conclusion can be drawn for prn 20 and 17. Two other satellites in view presented similar characteristics to the results for satellites prn 31 and 19. These were the satellites prn 32 and 28.

This leads to a second iteration for the 2nd step. A new receiver clock delay is estimated, without satellites prn 31, 19, 32, 28. The errors are computed again. The results are shown in Figure 7. It can be observed that multipath effects are already visible on satellites prn 20 and 17. It can be observed from Equation 6 that the estimation of the multipath on satellite i ($\Delta\hat{m}_i^v$) decreases due to NLOS multipath (a positive value) on others satellites, through the receiver clock estimation (expressed in Equation 4). Therefore, a distinction can be made on the origins of the errors observed on satellites prn 20 and 17. The negative errors on satellite prn 17 are due to the NLOS multipath on this satellite,

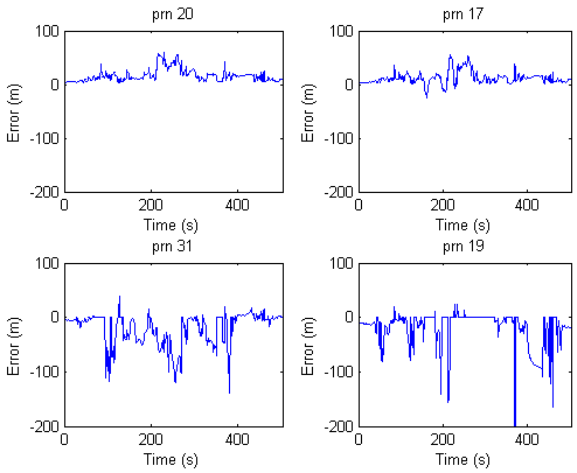

Fig. 6. Receiver autonomous method - 1st Iteration for the 2nd step

whilst positive errors on satellite prn 20 are mainly due to the NLOS multipath on the other satellites.

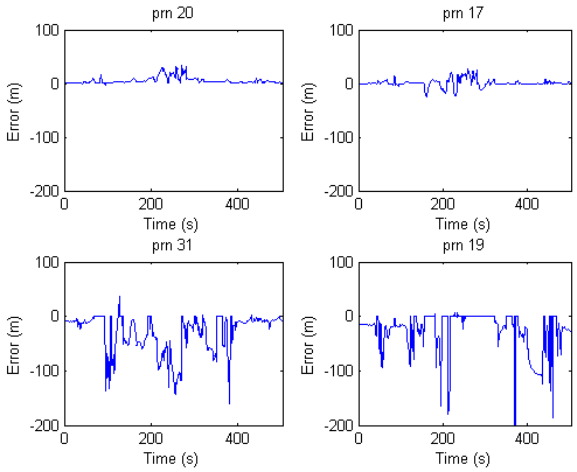

Fig. 7. Receiver autonomous method - 2nd Iteration for the 2nd step

Finally, a third iteration to estimate the receiver clock is made by taking into account only satellites prn 20 and 11 as these appear not to be submitted to multipath errors. This is compliant with the elevations of the satellites. The result leads to the error estimates shown in Figure 8. By visual inspection, there are no jumps for the pseudo range estimations of satellite prn 20, which is not the case for the other observed satellites. It is possible to infer that this satellite can be considered as fault free. A similar observation can be made with data from satellite 11.

For the double difference base method, Figure 9

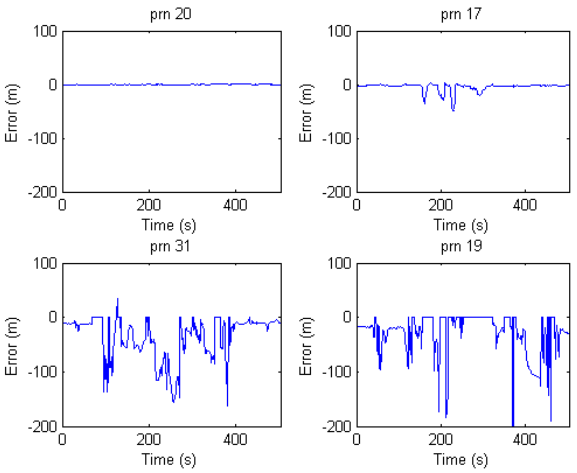

Fig. 8. Receiver autonomous method - 3rd Iteration for the 2nd step

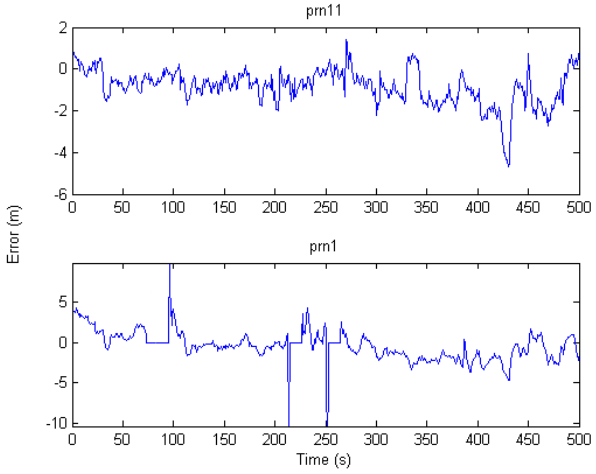

Fig. 9. Double difference method applied to satellite prn 11 and 1 with satellite prn 20 as reference

shows the pseudo-range computed for satellites prn 1 and 11 having satellite prn 20 as reference. Visual inspection of the lower plots leads to the conclusion that prn 20 and 11 are more than 95 % of the time fault free. By observing both plots it is possible to identify that for satellite prn 20 at $t = 430s$, and around $t = 340s$ for satellite prn 11 a fault occurs. Therefore one of these satellites can be taken as a reference for the double reference.

B. Comparison between the methods

The comparison is made on satellite 17 that proved to be affected by multipath. Figure 10 represents the difference of the errors computed with both methods on this satellite, with the GPS receiver set at 1 Hz.

The blue line represents the difference in pseudo-ranges errors and the red line the difference in the Doppler errors.

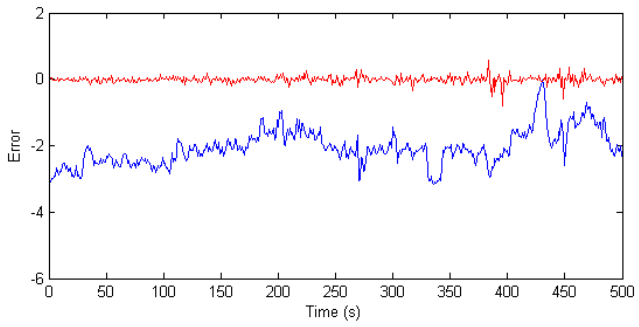

Fig. 10. Difference on the estimated errors by both methods

The first observation is that there is a bias in the difference of the pseudo-ranges, as this is not centered on 0. This observation, together with a check of the error plots from each method highlights the weakness of the third assumption used for the first method (the correction of atmospheric delays). In fact it is well known that atmospheric models and parameters broadcasted by the GPS are poor: their inaccuracy impacts the receiver clock offset estimation and consecutively multipath estimation. Secondly, one abrupt change can be observed around $t = 430s$. This is due to the multipath on satellite prn 20 used as reference satellite, as identified in the previous Section. There is no major difference when comparing the level of noise on the estimations.

It can be concluded that there are three major differences between both methods: First, the receiver autonomous method results in a bias in the absolute value of the pseudo-range error. This has only a moderate impact on multipath detection, because this is based on the observation of any abrupt change in this error. Second, the double difference based method requires only one fault free satellite. This is important as it can be applied to observations in densely built areas. Third, from an experimental perspective, the double difference method requires a reference station nearby, which is not always available.

C. Observation of Multipath

Figure 11 shows the pseudo-range errors on the pseudo-ranges for all the satellites in view during the recorded test trajectory. They were estimated using the double difference method with satellite prn 20 as reference. A constant amplitude was set for the

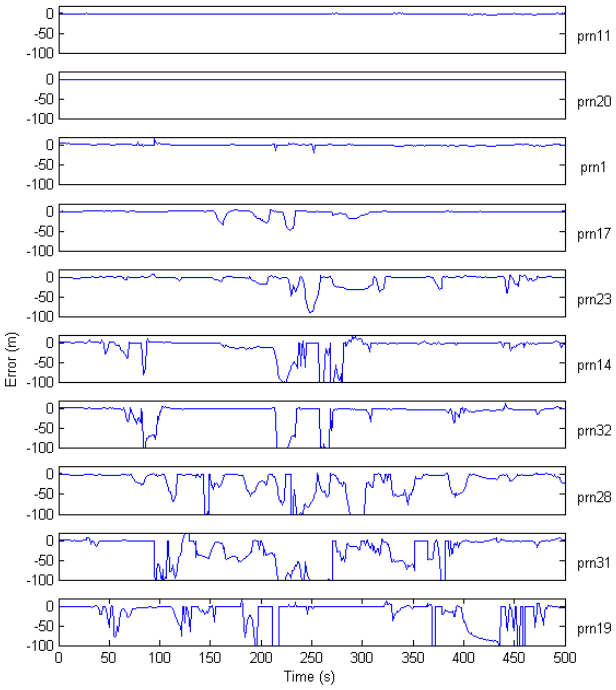

Fig. 11. Pseudo-range errors for all the GPS satellites in view

axis representing the error (between -100 m to +20 m) to provide the same scale despite the presence of errors with larger magnitudes. It can be observed that multiple errors exist due to multipath. Out of the 10 observed satellites only 2 (i.e. prn 11 and prn 20) can be considered as fault free during the whole trajectory. There are 3 satellites with very high errors (i.e. prn 28, 31 and 19), these can be considered as unusable during most of the vehicle trajectory as their errors can reach up to 200 m. Further, there are 5 satellites having errors larger than 50 m. These large magnitude can not be considered as originating from the addition of a direct signal plus a reflection. In a 10% narrow correlator the maximum delay is 0.025 chip, the equivalent of 7.5 m, in case of a 50% attenuated specular reflection [12]. Therefore the errors for these satellites should be considered as being mainly due to Non Line Of Sight (NLOS) multipath. This is the effect of only reflected signals as the direct ones are occluded.

Figure 12 presents the Doppler errors on all the observed satellites. These are estimated using the double difference method. The reference satellite is the one identified for the previous plot. The results are similar to the pseudo-ranges errors, as NLOS multipath impact

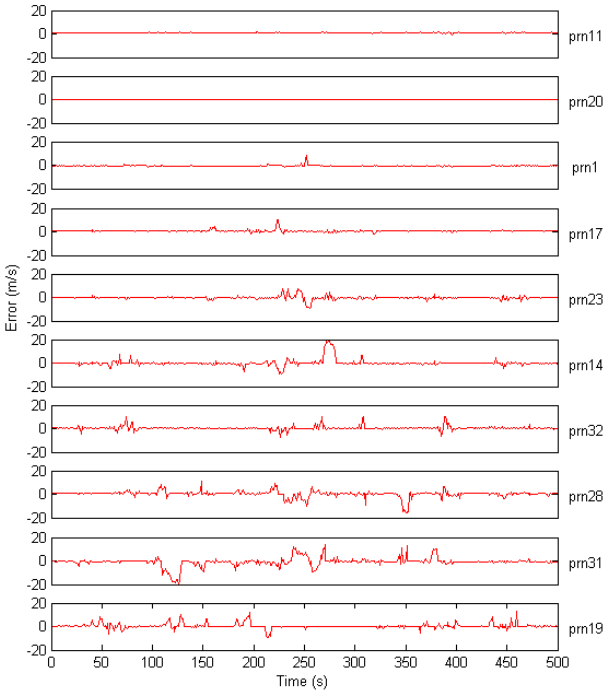

Fig. 12. Doppler errors for all the GPS satellites in view

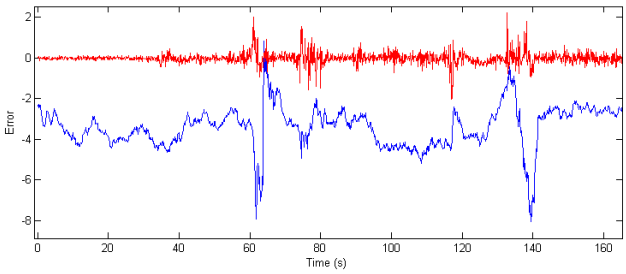

Fig. 13. Pseudo-range and Doppler errors at 10 Hz on satellite prn 17

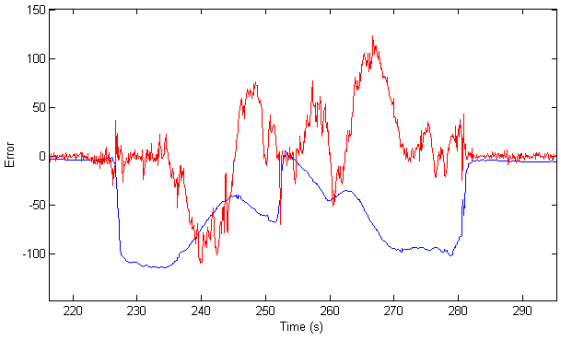

Fig. 14. Pseudo-range and Doppler errors at 10 Hz on satellite 32

both the pseudo-ranges and Doppler estimations. The time occurrence of errors is similar for a given satellite. Some errors reach up to 20 m/s in magnitude. If these are included in the estimation of the vehicle velocity and heading, they will lead to estimation errors.

Although the emphasis on the previous plots was the detectability of NLOS multipath, the effects of direct plus reflected signals can be also observed. Figure 13 represents the errors on satellite prn 17, from the GPS receiver configured at 10 Hz in order to have a better observation of the error dynamic. The errors were estimated using the autonomous receiver method, this explains the presence of the constant offset on the pseudo-range error. At time instants $t = 65s$ and $t = 135s$, two abrupt changes can be observed. Their magnitude of ± 4 m is compliant with the operation of a narrow correlator in the GPS receiver front-end. The effects of this multipath can be simultaneously observed on the pseudo-range and the Doppler errors.

It was observed that multipath affects both pseudo-range and Doppler measurements. Further, one can remark that, for NLOS multipath, the opposite of the Doppler error resembles to the derivative of the pseudo-range error, as it can be seen in Figure 14 between time $t = 230s$ and $t = 275s$. This relationship can be demonstrated by applying geometrical considerations, which are out of the scope of the paper. It is applicable only when the receiver tracks a reflected signal, but no longer valid during transitions.

The main purpose of the study is to acquire knowledge on the occurrence and the magnitude of multipath signals received at a GPS receiver on-board a passenger vehicle within an urban environment. The plots in Figures 11 and 12 show that the duration and the magnitude of NLOS multipath are the main source of GPS errors when traversing an urban environment. These lead to positioning errors whose amplitude may exceed 10 m in the XY plane. Although some faulty satellites can be identified with the help of their elevation or their SNR, there will be less than four fault-free satellites. Consequently, it will be impossible to estimate a correct position using a standalone GPS. Therefore means to detect these pseudo-range faults via Fault Detection and Exclusion algorithms specific to the automotive context are necessary [13].

D. 3D contextual analysis

Multipath exist due to the topographical relationship between the GPS receiver, the immediate environment

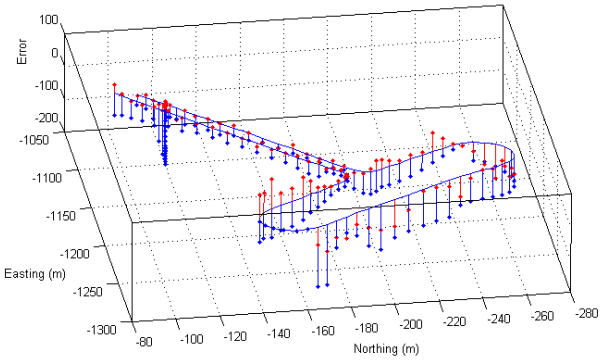

Fig. 15. 3D representation of pseudo-range and Doppler errors at 1 Hz on satellite 28

and the GPS satellite constellation. It is a 3D spatial problem. It is therefore very important to link the magnitude of the measured errors to the spatial location where they occur. The variations on pseudo-range and Doppler errors for the satellites prn 28 when the vehicle crosses one of the most challenging environments is shown in Figure 15. This is a 3D representation of the effects of multipath when the vehicle was traversing the Plaza showed in Figure 3. The results were recorded for a sampling interval of 1 Hz. The vehicle trajectory is the continuous line (in black), the vertical lines represent the errors projected in the true 2D trajectory of the vehicle. The blue lines represent the pseudo-range errors and the red lines Doppler errors. For visualization purposes, the magnitude of the Doppler error has been scaled up by a factor equal to 10. The interval at which the errors are plotted is at 1s The graph makes it possible to correlate the position of the vehicle with the associated errors due to multipath. The use of a 1 Hz sampling rate was found to be insufficient due to the speed at which the vehicle was travelling, it is difficult to identify the trends on the errors or any sudden jump.

By increasing the sampling rate to 10 Hz, it was observed that the trends on the errors could be observed much better, as shown in Figure 16 and 17. The first Figure relates the pseudo range and Doppler errors for satellite 32 in observed GPS constellation. This satellite was located towards the North-East, that is at the bottom left of the referred Figure. This location explains the higher error magnitudes measured when the vehicle runs alongside buildings near the entry to the Plaza. That is, the reflected signals bounce on opposite building, crossing the whole width of the Plaza towards the GPS receiver. When the vehicle is South West region of the Plaza, it travels near the reflecting source, the size of the multipath will be shorter and hence the error is lower. No multipath was detected when the vehicle outside the Plaza or when the vehicle is on the axis of the incoming road which coincides with the azimuth of the observed satellite, there is no occlusion.

The same type of reasoning can be applied to the results for satellite prn 23 shown in Figure 17. The satellite is located towards the South, that is to the left of the figure. It can then be understood the large error magnitude when the vehicle turns at the South part of the Plaza and on the road segment opposite to the entry of the Plaza. The position of the satellite and the curved shape of the building show the dynamics of the errors. That is, the undulations (slopes) on the pseudo-range errors, something which is not frequently observed in locations where the roads plus building architectures are straight.

The examples presented in the Figure show how contextual information facilitates the analysis of errors. These are linked to the position of the vehicle with respect to the azimuth and elevation of the satellite, and to the surrounding environment. The 3D information sampled at 10 Hz facilitates the interpretation of results.

E. Relation between errors and Signal Noise Ratio

The Signal Noise Ratio (SNR) is often used as an indication to identify multipath. The experimental results obtained have confirmed the presence of such correlation most of the time. Figure 18 presents the pseudo-range and Doppler errors on the upper part of graph, and the recorded SNR at the bottom. The receiver was configured to operate at 10 Hz, and the pseudo-range offset error is due to the use of the first method. The correlation is visible, for each error increase there is a decrease on the SNR. However, this observation is not always true, for example in Figure 19 at time $t = 170s$, a decrease of 10 dB can be observed without any change in the pseudo-range or Doppler error. Between $t = 188s$ and $t = 197s$, the pseudo-range has errors, this is due to some transients after reacquiring the good signal. At the same time, the SNR only decreases by 3 dB with respect to standard values.

The examples demonstrate the link between the SNR and multipath as well as the possible exceptions or difficult cases. It can be said that it is difficult to identify multipath using only SNR information. That is to reject pseudo-ranges affected by multipath based only on a fix SNR threshold will be difficult and could

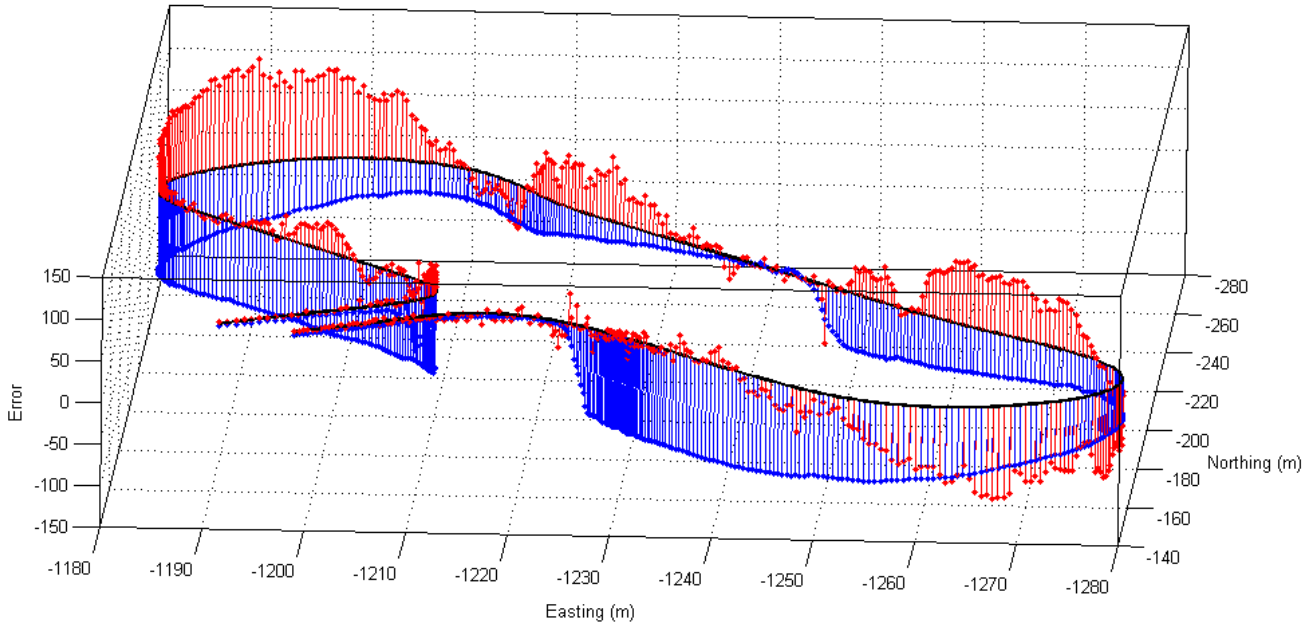

Fig. 16. 3D representation of pseudo-range and Doppler errors at 10 Hz on satellite 32

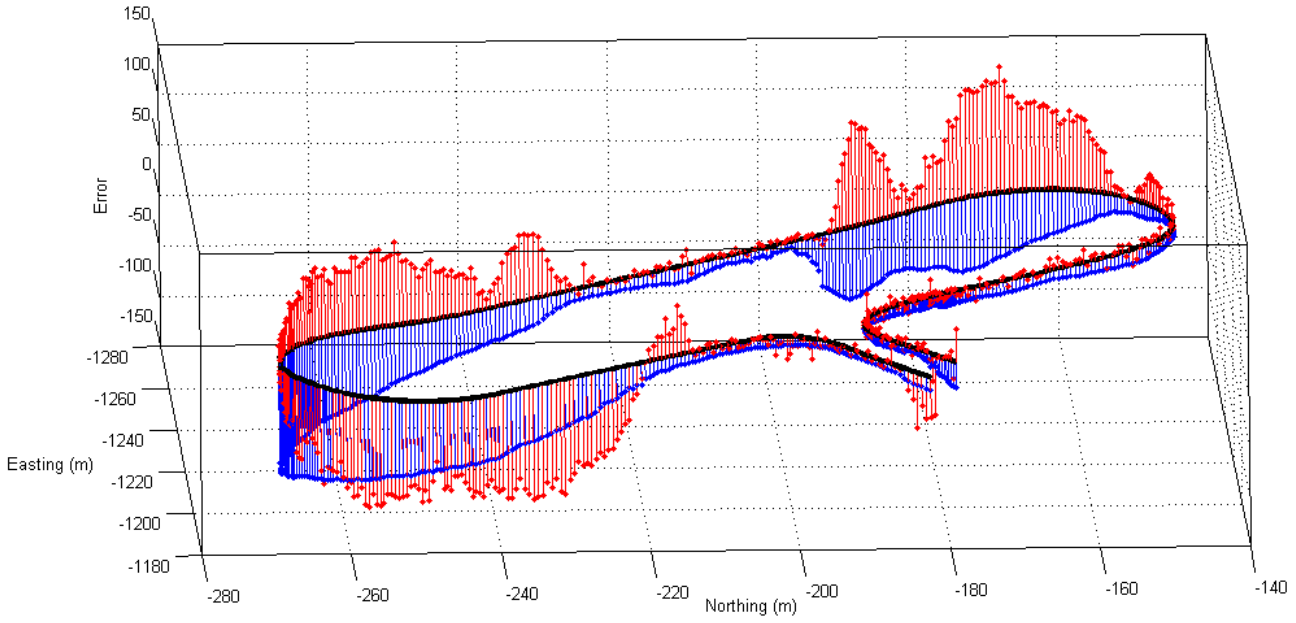

Fig. 17. 3D representation of pseudo-range and Doppler errors at 10 Hz on satellite prn 23

lead to position estimation errors.

CONCLUSION

The estimation of the vehicle position depends very much on pseudo-ranges and Doppler measurements, multipath affect directly the pseudo-ranges and thus the final estimated position. Future driving assistance applications will be very much dependent on position information, thus estimation errors would propagate to the applications and are likely to reduce performance. It is therefore necessary to gain an understanding of the effects of multipath for countermeasures to be designed and implemented. In this paper, two methods were proposed to characterize the effects of multipath when the GPS receiver is on-board of a moving vehicle

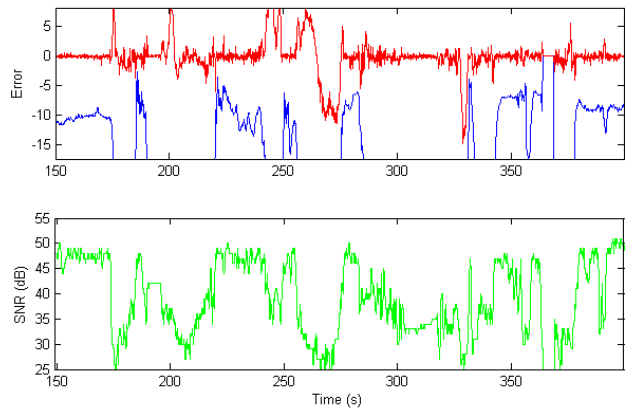

Fig. 18. Correlation between multipath and errors

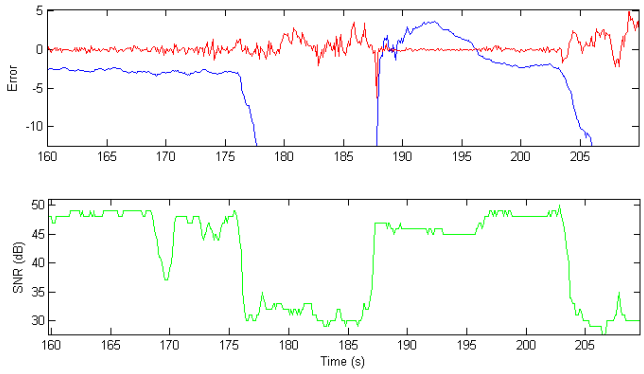

Fig. 19. Probable false alarms due to SNR

that traverses a dense urban environment. The first is based on a standalone solution using post-processing software to improve the quality of the measured reference position, whilst the second, needs of an additional reference base to provide the corrections. Both methods presents advantages and disadvantages, with results being similar. The selection of the methods depends on the available equipment and purpose of the study.

Analysis of the collected data showed the importance of NLOS multipath and the effects it has on the measurements made with the GPS receiver. The link between the signal to noise ratio and errors together with the possible weaknesses has been underlined. Further, the results have shown that there are multiple errors of large magnitude due to the physics encountered in urban environments. Therefore, it is necessary to apply algorithms that take into account the presence of multiple errors. The use of single fault detection algorithms such as RAIM will not be very suitable for this purpose. The results will permit the design of relevant countermeasures to palliate the effects of multipath like for example the use of fault detection and exclusion algorithms (FDE). It is now possible to identify the occurrence of pseudo-range errors due to multipath so as to evaluate the performance of the proposed FDE algorithms. By associating all errors with the environment in a 3D manner it is possible to gain a better understanding of the different relationships, between multipath, vehicle position and surrounding environment.

REFERENCES

[1] S. Feng and W. Ochieng, "Integrity of navigation system for road transport," in *Proc. 14th World Congress of Intelligent Transportation Systems*, Beijing, Oct. 2007.

[2] H. Durrant-Whyte, D. Pagac, B. Rogers, M. Stevens, and G. Nelmes, "An autonomous straddle carrier for movement of shipping containers," *IEEE J. Robot. Automat.*, vol. 14, pp. 14–23, Sep. 2007.

[3] J. Ibañez-Guzmán, O. Le Marchand, and C. Chen, "Metric evaluation of automotive-type GPS receivers," in *Proc. FISITA*, Munich, Germany, Sep. 2008.

[4] D. J. R. Van Nee, "Multipath effects on GPS code phase measurements," *NAVIGATION, Journal of Navigation*, vol. 39, no. 2, 1992.

[5] J. M. Kelly, M. S. Braasch, and M. F. DiBenedetto, "Characterization of the effects of high multipath phase rates in GPS," *GPS Solutions*, vol. 7, no. 1, pp. 5–15, May 2003.

[6] B. M. Hannah, "Modelling and simulation of GPS multipath propagation," Ph.D. dissertation, Queensland University of Technology, Queensland, Australia, 2001.

[7] G. Moura and J. Castets, "Validation of deterministic simulation of GNSS reception in urban areas by comparison with measurement campaign," in *Proc. of the European Navigation Conference GNSS*, Toulouse, France, Apr. 2008.

[8] L. Hagerman, "Effects of multipath on coherent and noncoherent ranging receivers," The Aerospace Corporation, Tech. Rep. TOR-0073 (3020-03)-3, May 1973.

[9] E. Kaplan, *Understanding GPS: Principles and Applications*. Artech House Publishers, Feb. 1996.

[10] IXSEA. LANDINS. [Online]. Available: http://www.ixsea.com/en/products/002.001.003.001/landins.html. [Accessed: Apr. 20, 2009]

[11] Novatel. Waypoint inertial explorer. [Online]. Available: http://www.novatel.com/products/waypoint_inertial.htm. [Accessed: Apr. 20, 2009]

[12] R. Van Nee, "Multipath and multi-transmitter interference in spread-spectrum communication and navigation systems," Ph.D. dissertation, Delft University of Technology, The Netherlands, 1995.

[13] O. Le Marchand, P. Bonnifait, J. Ibañez-Guzmán, F. Peyret, and D. Bétaille, "Performance evaluation of fault detection algorithms as applied to automotive localization," in *Proc. of the European Navigation Conference GNSS*, Toulouse, France, Apr. 2008.